CHEMICAL ENGINEERING TRANSACTIONS

VOL. 114, 2024

A publication of AIDIC
The Italian Association of Chemical Engineering
Online at www.cetjournal.it

Guest Editors: Petar S. Varbanov, Min Zeng, Yee Van Fan, Xuechao Wang

ISBN 979-12-81206-12-0; **ISSN** 2283-9216

DOI: 10.3303/CET24114068

Physics-Informed Neural Networks for Inversion of the Macroscopic Transport Parameters in Packed Bed

Mouhao Wang[a], Shanshan Bu[a,*], Bing Zhou[b], Baoping Gong[b], Zhenzhong Li[a], Deqi Chen[a]

[a]Key Laboratory of Low-Grade Energy Utilization Technologies & System, Chongqing University, Chongqing, China
[b]Southwestern Institute of Physics, Chengdu, 610225, China
shanshanbu@cqu.edu.cn

The effective permeability and effective thermal conductivity represent the macroscopic transport parameters crucial for characterizing fluid flow and heat transfer in packed beds. Accurately determining these parameters is essential for successful upscaling from the pore scale to the packed bed scale. In this study, a novel approach utilizing Physics-Informed Neural Networks (PINNs) is introduced to enhance the precision and efficiency in estimating these macroscopic transport parameters during the upscaling process. This approach treats the estimation of transport parameters as an inverse problem framed within the context of PINNs, where the network learns the underlying physical laws and outputs the desired macroscopic parameters. The minimization of discrepancies in pressure drops and temperature between the pore-scale and packed-bed scale models forms the basis of the objective function. The results demonstrate a high degree (relative deviations are within 1 %) of agreement between the pore-scale and packed-bed scale models in multi-physics fields, validating the effectiveness of the PINNs-based approach in accurately capturing the macroscopic transport parameters for packed beds. Macroscopic transport parameters of solid breeding blanket-packed beds in fusion reactors at different inlet velocities (0.05~0.25 m/s) and different inlet temperatures (300~900 K) are obtained.

1. Introduction

Flow and heat transfer in packed beds captivates engineering interest due to its broad practical applications in various fields. Examples include catalytic reactors (Shah et al., 2023), pebble bed reactors (Wu et al., 2023), thermal energy storage (He et al., 2023), solar receivers (Wei et al., 2024), and solid breeding blankets in fusion reactors (Gong et al., 2024). Understanding the heat and mass transfer dynamics is crucial for system design and evaluation. However, packed-bed systems vary greatly in spatial scale and have very complex internal structures, making pore scale analysis challenging. In engineering applications, macroscopic transport parameters, such as effective permeability and thermal conductivity, are often introduced to represent overall flow and heat transfer characteristics (Luo et al., 2020). These parameters could be directly used to simplify the pore scale model (Wang et al., 2023) to a packed-bed scale model (Wang et al., 2024) through the porous media approach to quickly evaluate the pressure drop and temperature distribution of the whole packed bed.

The determination of macroscopic transport parameters often relies on empirical correlation models. However, these models often overlook the complex interactions between fluid flow and heat transfer at the pore scale. For instance, models like Kozeny-Carman neglect the influence of heat transfer when calculating the effective permeability of packed beds, while models such as Chew-Glandt fail to consider internal flow within porous media when predicting effective thermal conductivity. These simplifications will not be reasonable in some practical applications (Wang et al., 2024). Particularly in industrial scenarios with significant temperature or pressure gradients, separately considering flow and heat transfer can overlook their mutual influences, potentially leading to biases in understanding and predicting the overall heat and mass transfer behaviors of packed beds.

Paper Received: 20 May 2024; Revised: 28 September 2024; Accepted: 12 November 2024
Please cite this article as: Wang M., Bu S., Zhou B., Gong B., Li Z., Chen D., 2024, Physics-Informed Neural Networks for Inversion of the Macroscopic Transport Parameters in Packed Bed , Chemical Engineering Transactions, 114, 403-408 DOI:10.3303/CET24114068

Recent advancements in machine learning, particularly the emergence of Physics-informed Neural Networks (PINNs), offer promising avenues for addressing these challenges (Raissi et al., 2019). By integrating principles of physics into neural network architectures, PINNs have demonstrated the capability to learn complex physical phenomena directly from data while respecting fundamental governing equations (Qiu et al., 2022). This paper focuses on leveraging Physics-informed Neural Networks for the inversion of macroscopic transport parameters in packed beds. Specifically, it aims to develop a novel approach that utilizes PINNs to infer macroscopic transport parameters directly from pore scale data coupling flow and heat transfer (Section 2). The method is used in Section 3 of this paper to test and obtain macroscopic transport characteristics within the solid breeding blanket-packed bed in a fusion reactor. This research provides a new way of thinking about the rapid design and evaluation of industrial-packed beds for computation.

2. Numerical method

2.1 Physical models

In this study, the helium-cooled solid blanket featuring a typical packed bed structure is used as a research object for the construction and testing of this approach. The previous extensive numerical simulations have examined flow and heat transfer within this blanket at both pore scale (Wang et al., 2023) and packed-bed scale (Wang et al., 2024), yielding reliable numerical methods for ongoing research. This study serves as a continuation of the prior research endeavors. As depicted in Figure 1, numerous Li_4SiO_4 pebbles (diameter $\boldsymbol{d}_p$= 1 mm) serve as tritium breeding material, randomly packed within the blanket to create a pebble-bed structure. Upon neutron irradiation, these pebbles undergo transmutation reactions, releasing heat outward, and the Li_4SiO_4 particles within the blanket act as heat under operational conditions. Helium gas flows upward from the bottom of the packed bed, forming a helium domain within the packed bed. This study focuses on a packed bed measuring $12.5\boldsymbol{d}_p \times 12.5\boldsymbol{d}_p \times 10\boldsymbol{d}_p$, with a porosity ($\varepsilon$) of 39.7 % to investigate macroscopic transport characteristics within the packed bed. The pore scale model accurately reproduces the pebbles and pores within the packed bed, while the packed-bed scale model replaces the packed bed region with a porous medium. Both scale models incorporate an inlet section ($10\boldsymbol{d}_p$) and an outlet section ($10\boldsymbol{d}_p$) to mitigate boundary effects.

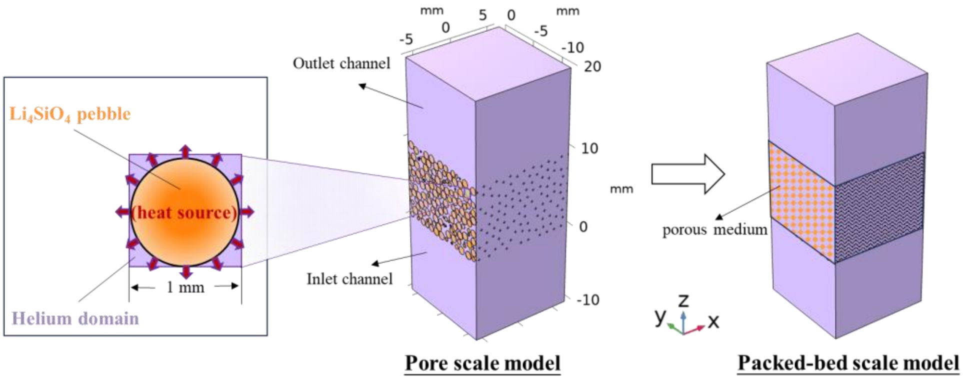

Figure 1: Pore-scale model and packed-bed scale model of solid breeding blanket packed bed

2.2 Governing equations and boundary conditions

Because of the low Reynolds number for solid breeding blanket design (*Re* ~ 1), the steady laminar flow is applied in this study. The control equations for flow and heat transfer are listed in Table 1. In these equations, $\boldsymbol{V}_f$ is the fluid velocity; p is the pressure; T is the temperature; ρ_f is the fluid density; μ is the fluid viscosity; C_p is the specific heat capacity; ϕ and ϕ_e (where ϕ_e= (1-ε)ϕ) are the internal heat source intensity and equivalent intensity. λ_f and λ_s denote the thermal conductivity of the fluid and solid. Additionally, κ_e and λ_e are the effective permeability and effective thermal conductivity of the packed bed, which represent the macroscopic transfer characteristic of the flow and heat transfer. The above equations are all solved by COMSOL software, and the boundary conditions are set in Figure 2, where the cooling wall temperature remains constant at 635 K from the packed bed to the outlet channel. However, to minimize inlet effects, the wall temperature matches the temperature of the helium inlet. Table 2 details the other operating parameters, with 20 different inlet conditions considered. The properties of helium and Li_4SiO_4 pebble are listed in Table 3.

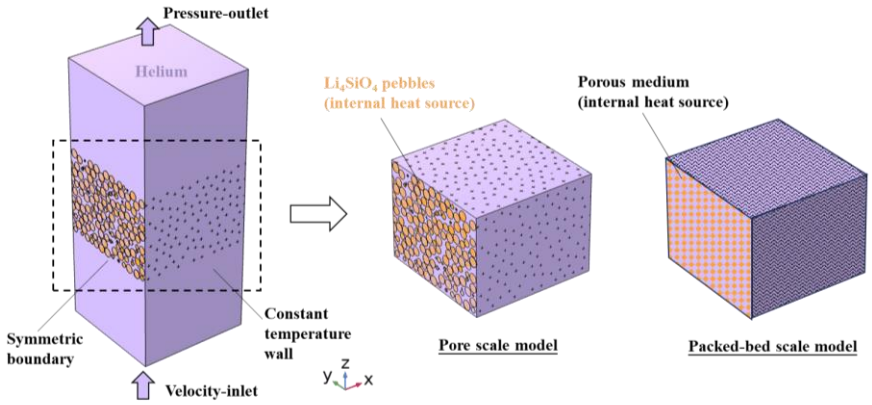

Figure 2: Boundary conditions setting

Table 1: The governing equations of the packed bed

	Pore scale model	Packed-bed scale model
For fluid flow	$\nabla\cdot(\rho_f \boldsymbol{V}_f)=0$	$\nabla\cdot(\rho_f \boldsymbol{V}_f)=0$
	$\rho_f(\boldsymbol{V}_f\cdot\nabla \boldsymbol{V}_f)=-\nabla p+\nabla\cdot(\mu\nabla \boldsymbol{V}_f)$	$\boldsymbol{V}_f=-\frac{K_e}{\mu}\nabla p$
For heat transfer	$\rho_f C_p(\boldsymbol{V}_f\cdot\nabla T)=\nabla\cdot(\lambda_f\nabla T)$ $\nabla\cdot(\lambda_s\nabla T)+\phi=0$	$\rho_f C_p(\boldsymbol{V}_f\cdot\nabla T)=\nabla\cdot(\lambda_e\nabla T)+\phi_e$

Table 2: Lists of the other operating parameters

Operating parameter	Value
Inlet velocity u_{in} (m·s^{-1})	0.05, 0.1, 0.15, 0.20, 0.25
Inlet temperature T_{in} (K)	300, 500, 700, 900
Internal heat source intensity ϕ (MW·m^{-3})	6.85
Working pressure (MPa)	0.12

Table 3: Lists of the physical properties (Wang et al., 2014)

Material	Physical property	Value
Helium gas	Density ρ_f (kg·m^{-3})	$480.19p/T$
	Viscosity μ (Pa·s)	$0.4646\times T^{0.66}\times10^{-6}$
	Thermal conductivity λ_f (W·m^{-1}·K^{-1})	$0.1448\times(T/273)^{0.68}[1+2.5\times10^{-3}p^{1.17}(T/273)^{-1.85}]$
	Specific heat capacity C_p (J·kg^{-1}·K^{-1})	5,200
Li_4SiO_4 particle	Density ρ_s (kg·m^{-3})	1,526.4
	Thermal conductivity λ_s (W·m^{-1}·K^{-1})	1.42

2.3 Numerical method validation

In prior study (Wang et al., 2023), numerous pore-scale simulations were conducted on the solid breeding blanket, validating the numerical method's reliability by assessing fluid flow and heat transfer characteristics. Figure 8(a) in that work illustrates the calculation of the pressure drop coefficient across the packed bed at inlet velocities of 0.05 m/s, 0.10 m/s, 0.15 m/s, 0.20 m/s, and 0.25 m/s, with relative deviations from the Blake-Kozeny-Macdonald equation below 1 %. Figure 8(b) displays the average Nusselt number, with calculations falling within 15 % of the well-established Wakao equation's predictions, valid for laminar flow.

3. PINNs model

3.1 PINNs for macroscopic transport parameters inversion

PINNs, as a deep learning method incorporating physical principles, construct a neural network by integrating governing equations, initial, and boundary conditions into the loss function, facilitating equation solution through optimization. By treating the coefficient as an optimization variable, PINNs enable coefficient inversion.

In this study, PINNs were employed to inversely calculate the effective permeability and effective thermal conductivity of the packed-bed scale model using pore scale model results as benchmark data. Figure 3 illustrates the physics-informed neural network for this inversion process. A fully-connected neural network is designed to capture the correlation between coordinates and physical attributes, expressed as Eq (1):

$$[u, v, p, T] = F_{NN}(X;\Theta) \tag{1}$$

Here, $X = (x, y)$ denotes the two-dimensional spatial variables inputted into the neural network. u and v represent the fractional velocities of $\boldsymbol{V}_{\mathrm{f}}$ in X and Y direction. $\Theta = (W, B, \kappa_{\mathrm{e}}, \lambda_{\mathrm{e}})$ encompasses the trainable parameters, consisting of weights, biases, and two macroscopic transport parameters. The neural network F_{NN} predicts the flow field and temperature field. The relationship between the n-th hidden layer and the (n-1)-th hidden layer is represented by Eq (2):

$$X^{n} = \sigma(W^{n-1}X^{n-1}+B^{n-1}) \tag{2}$$

Here, tanh function serves as the nonlinear activation function denoted by σ.

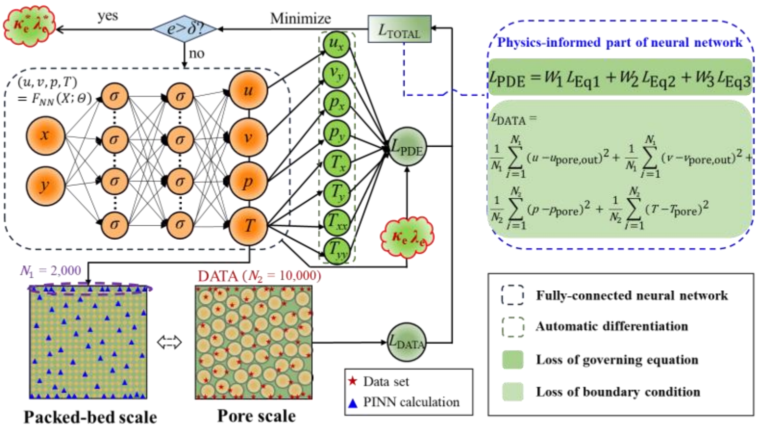

Figure 3: Illustration of physics-informed neural networks for macroscopic transport parameters of packed bed

The PINNs' total loss function comprises two components: the physics-informed part and the data-driven part. The physics-informed section of the neural network (Eqs (3)-(6)) originates from the governing equations of the packed-bed scale model.

$$L_{\mathrm{PDE}} = \omega_1 L_{\mathrm{Eq1}} + \omega_2 L_{\mathrm{Eq2}} + \omega_3 L_{\mathrm{Eq3}} \tag{3}$$

$$L_{\mathrm{Eq1}} = \rho_{\mathrm{f}} u_x + \rho_{\mathrm{f}} v_y \tag{4}$$

$$L_{\mathrm{Eq2}} = u + v + \frac{\kappa_{\mathrm{e}}}{\mu}(p_x + p_y) \tag{5}$$

$$L_{\mathrm{Eq3}} = \rho_{\mathrm{f}} C_{\mathrm{p}}\left(uT_x + vT_y\right) - \lambda_{\mathrm{e}}(T_{xx} + T_{yy}) - \phi_{\mathrm{e}} \tag{6}$$

Where L_{PDE} represents the loss incurred in partial differential equations (PDE), encompassing the loss associated with the continuity equation, momentum equation and energy equation, denoted as L_{Eq1}, L_{Eq2}, L_{Eq3}. ω_1, ω_2 and ω_3 are the weights of each loss which are 10^3, 1 and 10^{-19}, to guarantee the loss' values are in the same order of magnitude. u_x, v_y, p_x, p_y, T_x, T_y, T_{xx} and T_{yy} are the first and second-order partial derivatives of velocity, pressure and temperature with respect to variables x and y, which would be computed by automatic differentiation. The loss function (L_{DATA}) for the data-driven section utilized the mean squared error (MSE) to gauge the disparity between the model output (from PINNs) and the actual target value (from the pore scale model), as shown in Eq (7).

$$L_{\mathrm{DATA}} = \frac{1}{N_1}\sum_{i=1}^{N_1}(u - u_{\mathrm{pore,out}})^2 + \frac{1}{N_1}\sum_{i=1}^{N_1}(v - v_{\mathrm{pore,out}})^2 + \frac{1}{N_2}\sum_{j=1}^{N_2}(p - p_{\mathrm{pore}})^2 + \frac{1}{N_2}\sum_{j=1}^{N_2}(T - T_{\mathrm{pore}})^2 \tag{7}$$

Where the subscript 'pore' represents the calculation data from the pore scale model, 'out' denotes the data on outlet boundary; N_1 is the number of training data points on outlet boundary (N_1=2,000), N_2 is the number of training data points in the packed bed (N_2=10,000); i and j represent the data point's ordinal number. The overall loss function (L_{TOTAL}) can then be computed using Eq (8).

$$L_{\mathrm{TOTAL}} = \omega_{\mathrm{LED}} L_{\mathrm{PDE}} + \omega_{\mathrm{DATA}} L_{\mathrm{DATA}} \tag{8}$$

We utilized the Adam optimization method for stochastic optimization to minimize L_{TOTAL} during each network training iteration. ω_{LED} and ω_{DATA} are the weights of the PDE loss and data loss, which are 1 and 10^4. This optimizer fine-tunes the weights (W), biases (B) and macroscopic transport parameters (κ_e, λ_e) in PINNs network, leading to a decrease in the overall loss function. Once the training epoch (e) exceeds the specified value δ (δ = 60,000), the inversed macroscopic transport parameters are outputted.

3.2 PINNs model validation

In order to verify the inversion ability of the PINNs model, a packed bed scale model with given macroscopic transport parameters (κ_e = 9.95×10^{-10} m^2, λ_e = 0.35 W/(m·K)) is inversely calculated. As shown in Figure 4, the loss convergence of the model is good, and the deviations between the two inversed macroscopic transport parameters by PINNs and the given values are both within 1 %.

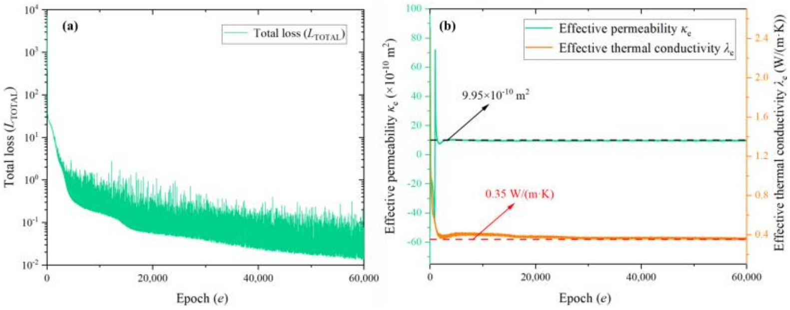

Figure 4: Validation of PINNs model: (a) loss convergence (b) macroscopic transport parameters convergence

4. Results and discussions

4.1 Macroscopic transport parameters inversion and field comparison

Using the PINNs model, the inversed effective permeability and effective thermal conductivity of solid blanket packed bed at u_{in}=0.05 m/s and T_{in}=700 K are 1.01×10^{-9} m^2 and 0.76 W/(m·K). Then the inversed macroscopic transport parameters are substituted into the packed-bed scale model for calculation and compared with the results of the pore scale model. As shown in Figure 5(a) which exhibits the pressure contours on the packed-bed midsection (Z=6.25d_p), the pressure distributions with pore-scale model and packed-bed scale model are very close, and the pressure drops are both 21.4 Pa. Figure 5(b) shows that the temperature distribution with the packed-bed scale model is almost as same as that with pore-scale model and the maximum temperature deviation between the two is only 3 K (within 1 %). These comparisons could further illustrate the effectiveness of the macroscopic transport parameters obtained by PINNs inversion.

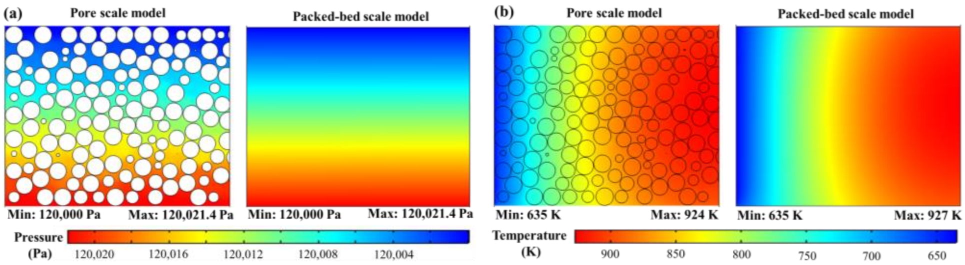

Figure 5: Comparison between pore scale model and packed-bed scale model of (a) pressure distribution and (b) temperature distribution at u_{in}=0.05 m/s and T_{in}=700 K

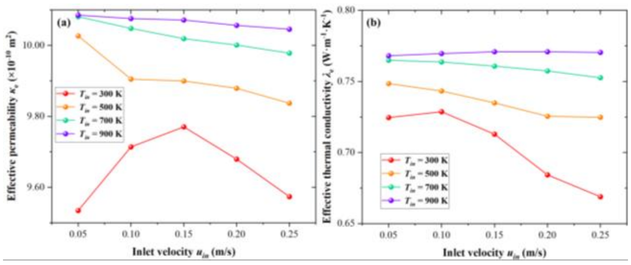

Figure 6: Macroscopic transport parameters comparison: effective (a) permeability (b) thermal conductivity

4.2 Macroscopic transport parameters at different working conditions

Figure 6 compares macroscopic transport parameters at different work conditions (u_{in}=0.05~0.25 m/s and T_{in}=300~900 K). In general, effective permeability and effective thermal conductivity increase as the inlet temperature increases because the higher packed-bed temperature makes the viscosity and thermal conductivity of the helium greater. However, the changing trend of the macroscopic transport parameters of the pebble bed with the increase of the helium flow rate in the pebble bed is not obvious, which is due to the inconsistent temperature field of the packed bed.

5. Conclusion

The effective permeability and thermal conductivity are pivotal macroscopic transport parameters for characterizing fluid flow and heat transfer in packed beds. This study presents a novel approach employing Physics-Informed Neural Networks (PINNs) to estimate these macroscopic transport parameters during upscaling. The estimation of transport parameters is framed as an inverse problem within the PINNs framework, enabling the network to learn underlying physical laws and generate the desired macroscopic transport parameters. With macroscopic transport parameters by PINNs, a packed-bed scale model is of substantial agreement with the pore-scale model across multiple physics domains, and relative deviations are 1 %, affirming the efficacy of this PINNs-based approach. Furtherly, macroscopic transport parameters of solid breeding blanket-packed beds in fusion reactors at different inlet velocities (0.05~0.25 m/s) and different inlet temperatures (300~900 K) are obtained. This study provides new ideas for the evaluation of the fluid-heat transfer performance of industrial-packed beds.

Acknowledgments

We would like to acknowledge financial supports for this work provided by the National Natural Science Foundation of China (No. 52276052).

References

Gong B., Cheng H., Zhou B., Yan J., Wang L., Zhang L., Feng Y., Wang X., 2024, Investigation of Wall Effect on Packing Structures and Purge Gas Flow Characteristics in Pebble Beds for Fusion Blanket by Combining Discrete Element Method and Computational Fluid Dynamics Simulation. Applied Sciences, 14(6), 2289.

He X., Qiu J., Wang W., Hou Y., Ayyub M., Shuai Y., 2023, Optimization design and performance investigation on the cascaded packed-bed thermal energy storage system with spherical capsules. Applied Thermal Engineering, 225, 120241.

Luo J.-W., Chen L., Min T., Shan F., Kang Q., Tao W., 2020, Macroscopic transport properties of Gyroid structures based on pore-scale studies: permeability, diffusivity and thermal conductivity. International Journal of Heat and Mass Transfer, 146, 118837.

Qiu R., Huang R., Yao X., Wang J., Zhang Z., Yue J., Zeng Z., Wang Y., 2022, Physics-informed neural networks for phase-field method in two-phase flow. Physics of Fluids, 34, 052109.

Raissi M., Perdikaris P., Karniadakis G.E., 2019, Physics-informed neural networks: A deep learning framework for solving forward and inverse problems involving nonlinear partial differential equations. Journal of Computational Physics, 378, 686-707.

Shah M., West D., Balakotaiah V., 2023, Analysis of thermoflow instabilities in adiabatic packed-bed catalytic reactors. Chemical Engineering Journal, 452, 139365.

Wang W., Cheng D., Feng K., Den H., 2014, Numerical simulation on thermal hydraulics characteristics of breeder pebble bed for China HCCB-TBM. Nuclear Fusion and Plasma Physics, 34(3), 200-206. (in Chinese)

Wang M., Bu S., Zhou B., Gong B., Li Z., Chen D., 2023, Pore-scale simulation on flow and heat transfer characteristics in packed beds with internal heat sources at low Reynolds numbers. International Journal of Heat and Mass Transfer, 213, 124325.

Wang M., Bu S., Zhou B., Gong B., Li Z., Chen D., 2024, Macroscopic transport characteristics in packed bed with a multi-physics inversion strategy for solid breeding blanket of HCCB TBM. Applied Thermal Engineering, 247, 123114.

Wei Y., Gao Z., Cheng Z., He Y., Zhang J., 2024, Comprehensive study on parabolic trough solar receiver-reactors via a novel efficient optical-thermal-chemical model of catalyst packed bed characteristics. International Journal of Hydrogen Energy, 49, 877-891.

Wu Z., Yang J., Wang Q., 2023, Numerical Investigation of Methane Steam Reforming in the Packed Bed Installed with Metal Foam. Chemical Engineering Transactions, 103, 67-72.